Journal of *Marine Science and Engineering*

MDPI

Article

Multifractal Analysis of the Structure of Organic and Inorganic Shale Pores Using Nuclear Magnetic Resonance (NMR) Measurement

Rui Yang [1,2], Weiqun Liu [2,*] and Lingren Meng [3]

[1] College of Civil Engineering and Architecture, Shandong University of Science and Technology, Qingdao 266590, China; ruiyang.bles@gmail.com
[2] State Key Laboratory for Geomechanics and Deep Underground and Engineering, China University of Mining and Science, Xuzhou 221116, China
[3] College of Energy and Mining Engineering, Shandong University of Science and Technology, Qingdao 266590, China
* Correspondence: weiqun_liu@126.com

Abstract: The multifractal structure of shale pores significantly affects the occurrence of fluids and the permeability of shale reservoirs. However, there are few studies on the multifractal characteristics of shale pores that distinguish between organic and inorganic pores. In this study, we obtained the pore size distribution (PSD) of organic and inorganic shale pores separately by using a new NMR-based method and conducted a multifractal analysis of the structure of organic and inorganic shale pores based on PSD. We then investigated the geological significance of the multifractal characteristics of organic and inorganic shale pores using two multifractal characteristic parameters. The results showed that the structures of both organic and inorganic pores have multifractal characteristics. Inorganic pores have stronger heterogeneity and poorer connectivity compared to organic pores. The multifractal characteristics of inorganic pores significantly affect shale permeability and irreducible water saturation. Greater heterogeneity in the inorganic pore structure results in lower shale permeability and higher irreducible water saturation. Meanwhile, better connectivity leads to higher shale permeability and lower irreducible water saturation. The multifractal characteristics of organic pores significantly affect the shale adsorption capacity and have a weak impact on irreducible water saturation. Greater heterogeneity in the organic pore structure results in the shale having stronger adsorption capacity and higher irreducible water saturation The results also indicate that the multifractal characteristic parameters of inorganic pores can be regarded as an index for estimating the irreducible water saturation and flowback rate of fracturing fluid, and the multifractal characteristic parameters of organic pores can be regarded as an index for evaluating the quality of shale reservoirs.

Keywords: shale reservoir; organic and inorganic pores; permeability; multifractal; geological significance

check for updates

Citation: Yang, R.; Liu, W.; Meng, L. Multifractal Analysis of the Structure of Organic and Inorganic Shale Pores Using Nuclear Magnetic Resonance (NMR) Measurement. *J. Mar. Sci. Eng.* **2023**, *11*, 752. https://doi.org/10.3390/jmse11040752

Academic Editor: George Kontakiotis

Received: 7 March 2023
Revised: 26 March 2023
Accepted: 27 March 2023
Published: 30 March 2023

Copyright: © 2023 by the authors. Licensee MDPI, Basel, Switzerland. This article is an open access article distributed under the terms and conditions of the Creative Commons Attribution (CC BY) license (https://creativecommons.org/licenses/by/4.0/).

1. Introduction

Due to the sustained growth of global energy demand, unconventional shale formations (including shale oil and shale gas) have received extensive attention in recent years as a major source of hydrocarbon production [1–3]. In contrast to conventional sandstone and carbonate formations, shale formations generally develop considerable nanoscale pore throats and possess stronger heterogeneity [4], which significantly affects formation permeability and the migration mechanisms of geofluids [5,6]. Therefore, characterizing the heterogeneity of shale pores is a crucial step in modeling shale gas recovery (SGR) or shale oil recovery (SOR).

Currently, conventional fractal and multifractal theories are the most commonly used methods to investigate the heterogeneity of shale pores. In terms of conventional fractal analysis of shale pores, previous studies have yielded significant findings. Firstly, numerous

experimental data and calculation results have proved that the PSD of shale exhibits obvious conventional fractal characteristics, with a conventional fractal dimension of between 2 and 3 [7–10]. Secondly, several potential factors may influence the fractal dimension of shale PSD, such as TOC [11], porosity [12], mineral content [13], and so on. Thirdly, the fractal dimension of shale PSD also affects the formation permeability and adsorption capacity of shale to some degree [7,14]. Xi et al. [5] and Yang et al. [11] found a negative correlation between shale permeability and the fractal dimension of shale PSD, while Ji et al. [9] and Xi et al. [5] suggested a positive correlation between the adsorption capacity of shale and the fractal dimension of shale PSD.

Besides the conventional fractal analysis, multifractal analysis is another powerful method that can provide further insights into the heterogeneity of shale pores. Liu et al. [3,15,16], Wang et al. [17] and Sun et al. [18] conducted multifractal analysis of shale pores using various techniques, including mercury intrusion porosimetry (MIP), gas adsorption, small angle scattering (SAS), scanning electron microscope (SEM) and nuclear magnetic resonance (NMR). Their analysis results indicated that shale PSD exhibits multifractal characteristics. Guan et al. [19] found that TOC has a strong impact on the multifractal parameters of shale PSD, while mineral content, thermal maturity and organic matter type show weak associations with the multifractal parameters of shale PSD. Liu et al. [15] compared the multifractal behavior of shale micropores and shale meso-macropores and found that the micropores exhibit better connectivity and weaker heterogeneity.

It is widely acknowledged that shale pores are highly complex and can be classified into two categories based on their substance composition: organic pores and inorganic pores [20–22]. Organic shale pores, which exhibit strong hydrophobic properties, offer ample space for adsorbed gas [8]. Understanding the characteristics of organic shale pores is crucial for studying the behavior of gas adsorption–desorption and assessing the shale gas reserves of reservoirs [23,24]. On the other hand, inorganic shale pores, which exhibit strong hydrophilic properties, serve as one of the primary channels for geofluids flow [25]. Determining the characteristics of inorganic shale pores is crucial for investigating water distribution and modeling the migration process of the gas phase and the water phase during SGR [6,26]

From the brief overviews above, it can be inferred that separate analysis of organic and inorganic shale pores for fractal characteristics (including conventional fractal characteristics and multifractal characteristics) may have important significance. However, at present, there have been only limited research reports in this specific field. Li et al. [27] and Zhang et al. [28] compared the fractal dimensions of organic and inorganic shale pores using SEM, and all the results showed that the fractal dimension of organic pores is larger than that of inorganic pores. Wang et al. [17] also separately investigated the heterogeneity of organic and inorganic shale pores using SEM digital images. Based on the fractal analysis, these researchers found that the inorganic shale pores possessed more obvious heterogeneity, which is contrary to the conclusion of Li et al. [27] and Zhang et al. [28]; based on the multifractal analysis, they found that the organic pores had better connectivity. From these limited studies, two shortcomings can be identified. The first is that all previous studies adopted SEM and image recognition technology to conduct the separate fractal analyses of organic and inorganic shale pores. This means that the scale of investigated samples is very small, which may increase the contingency of test results and induce further inconsistency in the analyses conclusions. The second is that a comprehensive comparison of the multifractal characteristics of organic and inorganic shale pores and of their geological significance is still lacking.

To address the research gaps mentioned above, this study categorically evaluates the fractal and multifractal characteristics of both organic and inorganic shale pores using NMR. The use of NMR is widely acknowledged as a non-invasive and non-destructive method to determine the PSD of centimeter-scale rock samples [29–31]. The primary objectives of this study are (1) to estimate the size distribution of both organic and inorganic shale pores, separately; (2) to assess the heterogeneity and connectivity of organic and

inorganic pores using multifractal theory; (3) to compare the multifractal parameters of organic and inorganic pores and (4) to discuss the geological significance of the multifractal characteristics of organic and inorganic shale pores.

2. Materials and Methods

2.1. Samples

In this study, six shale samples, numbered SC-1, SC-2, CQ-1, CQ-2, JX-1 and JX-2, were collected from the Sichuan Basin (located in Sichuan Province and Chongqing municipality, China) and the Jiurui basin (located in Jiangxi Province, China) to investigate the fractal and multifractal characteristics of organic and inorganic shale pores. The locations of the samples collected from the Sichuan basin are depicted in Figure 1: SC-1 and SC-2 were collected from Guangyuan city in Sichuan Province, and CQ-1 and CQ-2 were collected from the Fuling district in Chongqing. Additionally, to meet the testing requirement for NMR, all the samples were processed into a cylinder measuring 50 mm in length and 25 mm in diameter.

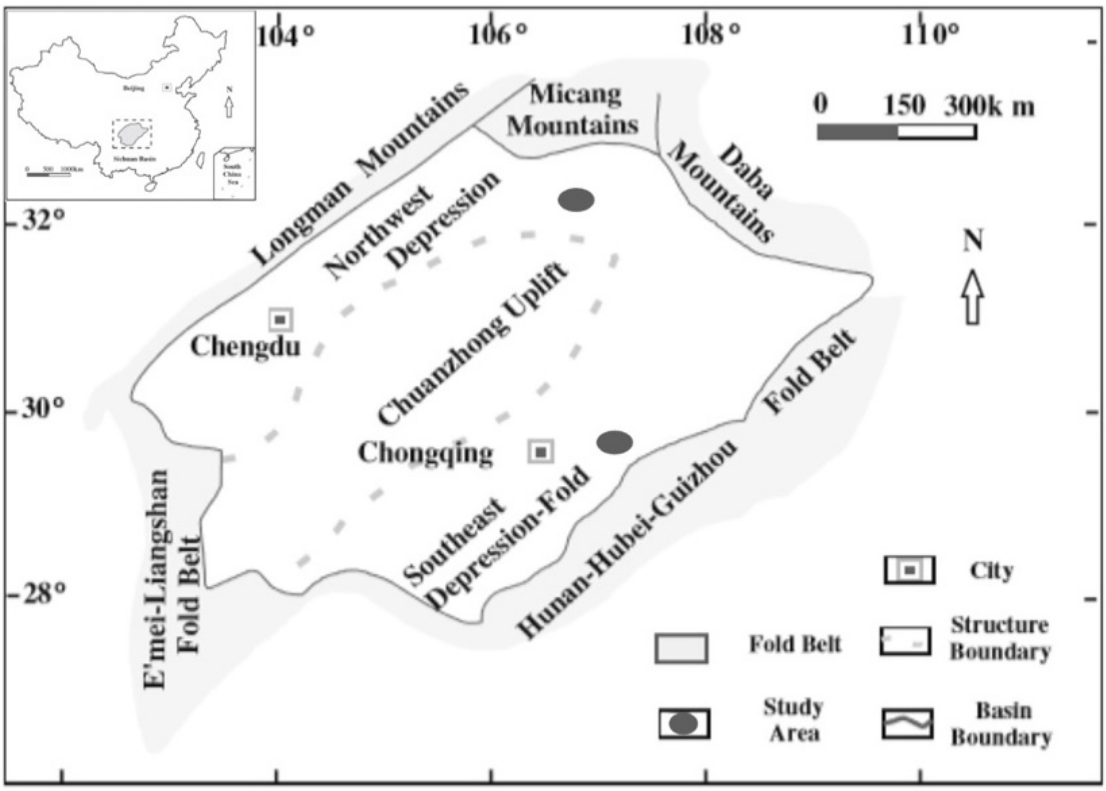

Figure 1. Locations of samples collected from the Sichuan Basin (modified from Wang et al. [32] and Liu et al. [33]).

2.2. Mineralogy and Geochemistry Analysis

A D8 ADVANCE X-ray diffractometer (XRD) was used to study the mineralogical content of the samples. The scanning measurements were performed at the rate of 2°/min in the range of 3–90° [15]. Then, the mineral percentages were estimated by calculating the curve of major peaks, and the results are listed in Appendix A Table A1. The TOC of the shale samples was tested using a LECO experimental instrument, which involved the following procedures: firstly, we pulverized shale samples into powders with granularity greater than 200 mesh and then soaked them with enough dilute hydrochloric acid to completely remove the inorganic carbon. Subsequently, distilled water was used to eliminate the residual hydrochloric acid in the samples, which could have damaged the detector in the instrument and caused result deviation. Finally, the processed samples were placed in a copper vessel that was suitable for use in the LECO instrument's combustor to determine

the TOC, and the results are listed in Appendix A Table A2. In the next step, the Ro of the shale samples was determined by measuring graptolite reflectivity [34], and the results are listed in Appendix A Table A2. The detailed test procedures and calculation methods used can be found in [35].

2.3. Nuclear Magnetic Resonance (NMR) Test

Plotting the PSD curve is imperative for analyzing the multifractal characteristics of rock pore structure. In this study, we separately determined the size distribution of organic and inorganic shale pores using a novel NMR-based method [22,36]. In this method, NMR experiments were conducted on shale samples under water- and kerosene-saturated conditions, respectively, and the detailed NMR measurement procedures are illustrated in Figure 2. The key experimental parameters and experimental conditions are as follows: number of scans, 32; echo spacing, 0.15 ms; waiting time, 6 s; resonance frequency, 12 MHz; echo numbers, 1024; temperature, 23.4 °C; humidity, 55.1%. Based on the wettability difference between organic shale pores and inorganic shale pores, the NMR test results under water-saturated conditions can reflect the size distribution of inorganic pores, while the NMR test results under kerosene-saturated conditions can reflect the size distribution of organic pores to a certain extent. Additionally, the quantitative relationship between pore size and relaxation time (T_2) obtained from NMR testing is described in the work of Li et al. [37] and, thus, will not be reiterated here. This method is suitable for analyzing inorganic shale pores measuring less than 5 μm and organic pores measuring less than 1.6 μm.

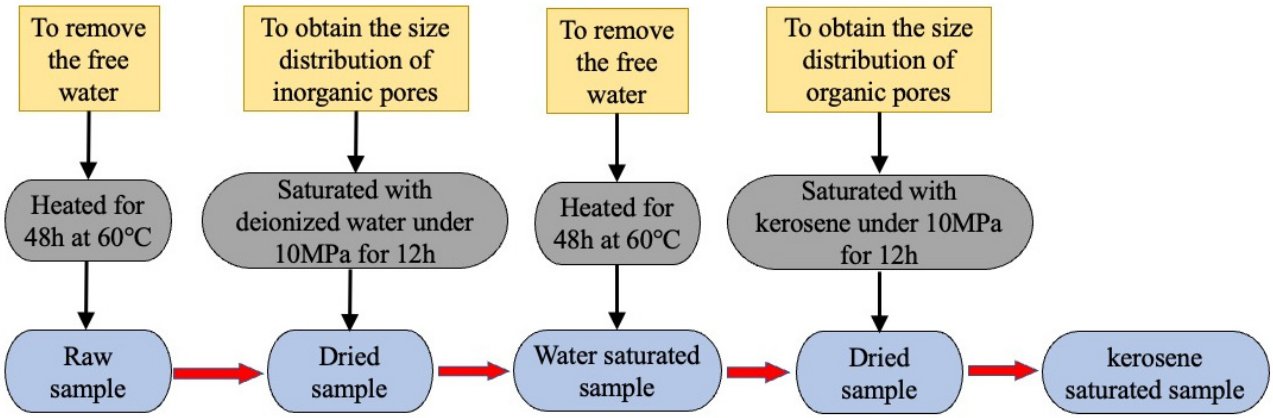

Figure 2. Detailed nuclear magnetic resonance measurement procedures and their purposes.

2.4. Multifractal Analysis

In this study, we used a box-counting method to conduct multifractal analysis on the PSDs of organic and inorganic shale pores. Box-counting techniques are commonly used for analyzing fractal properties of complex systems, such as porous materials [37–39]. In our approach, we divided the PSD into N subsets with equal pore size range ε and calculated the probability distribution function $P_i(i)$ of ith subset in universal set. This allowed us to analyze the multifractal properties of the shale pore structure and better understand the heterogeneity of organic and inorganic pores. Multifractal analysis is a powerful tool for quantifying the complex geometries and properties of natural materials [40–42] and can help improve our understanding of shale reservoirs and their potential for oil and gas extraction. The equation used is the following:

$$P_i(\varepsilon) = \frac{N_i(\varepsilon)}{N_T} \quad (1)$$

where $N_i(\varepsilon)$ is the pore volume of ith subset and N_T is the total pore volume. According to probability concepts, the relationship between $P_i(\varepsilon)$ and ε can also be expressed as:

$$P_i(\varepsilon) \propto \varepsilon^{\alpha} \tag{2}$$

where α is a singular index, which reflects the distribution heterogeneity of pore volume. If we denote the number of subsets with the same probability in the subsets labeled with α as $N_\alpha(\varepsilon)$, we can observe that as ε increases, the number of subsets also increases while $N_\alpha(\varepsilon)$ decreases. This relationship can be expressed by the following equation:

$$N_\alpha(\varepsilon) \propto \varepsilon^{-f(\alpha)} \tag{3}$$

where $f(\alpha)$ represents the fractal dimension of subsets labeled with α.

In the actual calculation process, the above equations are difficult to solve directly. Therefore, it is necessary to define an assignment equation to obtain the multifractal curve, which can be written as:

$$X_q(\varepsilon) \equiv \sum P_i(\varepsilon)^q \sim \varepsilon^{\tau(q)} \tag{4}$$

where $\tau(q)$ is the mass index, q is in the range of $-\infty < q < +\infty$. When the absolute value $|q|$ reaches a certain point, the multifractal curve tends towards stability. Therefore, q is typically limited to a certain range when performing calculations, and the specific bounds depend on the property of the research object. In this study, q was limited to the range of -10 to 10. By taking the logarithm of both sides of Equation (4), we obtain the following equation:

$$\tau(q) = \lim_{\varepsilon \to 0} \frac{\ln X_q(\varepsilon)}{\ln \varepsilon} \tag{5}$$

The theoretical expressions of α and $f(\alpha)$ can be calculated using the Legendre transformation, as follows:

$$\alpha = \frac{\mathrm{d}(\tau(q))}{\mathrm{d}q} = \frac{\mathrm{d}}{\mathrm{d}q}\left(\lim_{\varepsilon \to 0} \frac{\ln X_q(\varepsilon)}{\ln \varepsilon}\right) \tag{6}$$

$$f(\alpha) = \alpha q - \tau(q) \tag{7}$$

Additionally, according to Liu et al. [15], the generalized dimension (D_q), which characterizes the pore distribution complexity with the corresponding size, can be defined as follows:

$$D_q = \frac{\tau(q)}{q-1} \tag{8}$$

When $q = 1$, D_q will become

$$D_1 = \lim_{\varepsilon \to 0}\left(\sum \frac{P_i(\varepsilon)\ln P_i(\varepsilon)}{\ln(\varepsilon)}\right) \tag{9}$$

3. Results

3.1. Estimation of Size Distribution of Organic and Inorganic Pores in Shale

Based on the NMR test, the size distributions of the organic and inorganic pores of six shale samples are depicted in Figure 3. It is evident that the size of organic pores in shale is generally smaller than that of inorganic pores. In addition, as reported by Zhang et al. [22], the organic porosity (OP) and the inorganic porosity (IOP) can be calculated using the two T_2 curves obtained from water-saturated and kerosene-saturated shale samples. The calculation results for the shale samples in this study are listed in Table 1, and the mathematical equations used can be found in Zhang et al. [22].

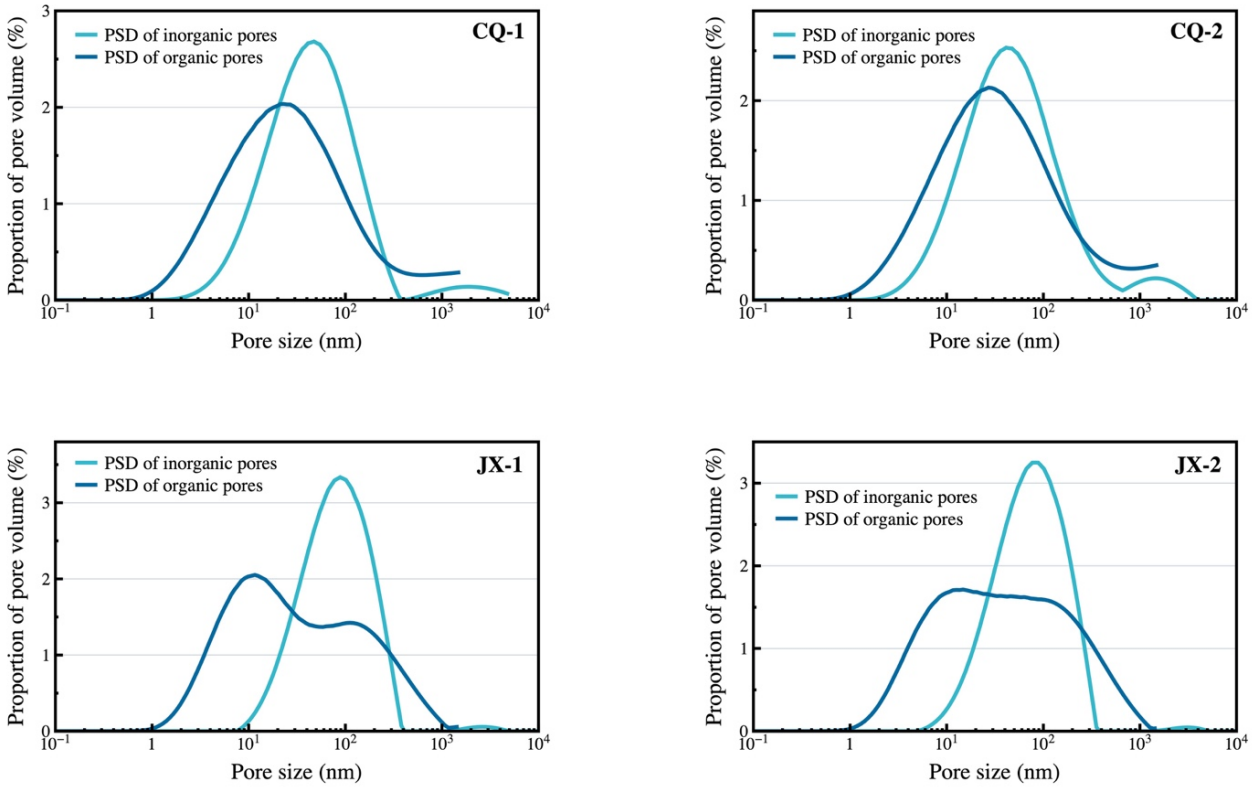

Figure 3. Size distributions of organic pores and inorganic pores in shale samples.

Table 1. Organic porosity (OP) and inorganic porosity (IOP) of the investigated shale samples.

Shale No.	Total Porosity	OP	IOP	Proportion of OP	Proportion of IOP
SC-1	2.38%	1.03%	1.35%	43.28%	56.72%
SC-2	2.58%	1.14%	1.44%	44.19%	55.81%
CQ-1	3.48%	1.63%	1.85%	46.93%	53.07%
CQ-2	3.82%	1.81%	2.01%	47.27%	52.73%
JX-1	1.11%	0.55%	0.56%	49.46%	50.54%
JX-2	1.16%	0.54%	0.62%	46.79%	53.21%

3.2. Method Comparison

Bringing the data of Figure 3 into Equations (6)–(9), the conclusions of the multifractal analysis can be drawn, as depicted in the plots shown in Figures 4 and 5.

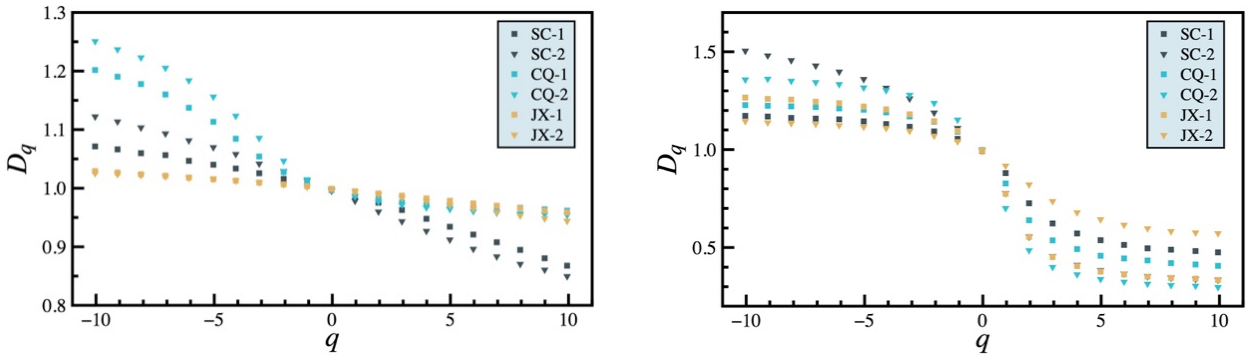

(**a**) (**b**)

Figure 4. Generalized fractal spectra of shale pores: (**a**) organic pores, (**b**) inorganic pores.

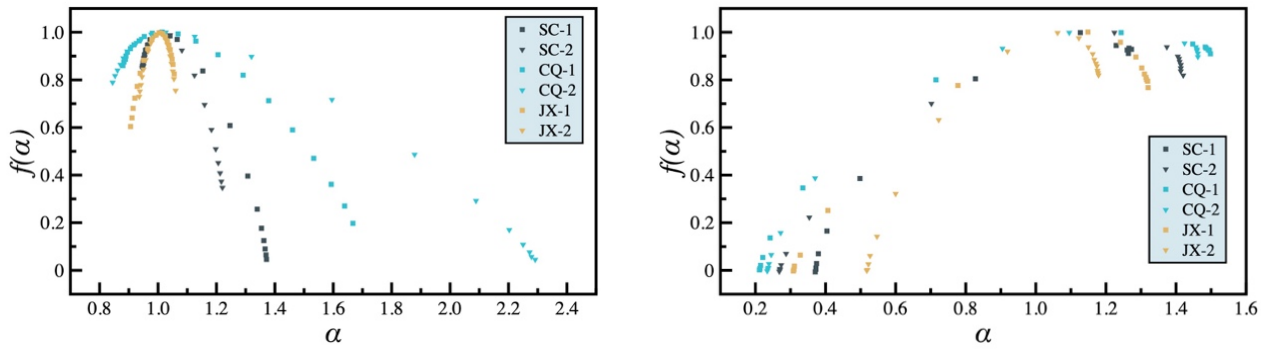

Figure 5. Multifractal spectra of shale pores: (**a**) organic pores, (**b**) inorganic pores.

Figure 4 illustrates the generalized fractal spectra (the relationship between D_q and q) of organic and inorganic shale pores, which describe the multifractal characteristics of pores with different sizes. D_q corresponding to smaller q mainly reflects the characteristics of seepage pores, while D_q corresponding to greater q mainly reflects the characteristics of adsorption pores. From Figure 4, it can be seen that D_q decreases with q for both organic pores and inorganic pores. To comprehensively analyze the generalized fractal spectra, several characteristic parameters were introduced in this study. These parameters include D_0, D_1, D_2, D_{qmax}, D_{qmin}, ΔD_q, $D_0 - D_1$ and H, where D, D_1 and D_2 represent the generalized dimension when $q = 0$, 1 and 2, respectively, D_{qmax} and D_{qmin} are the maximum and minimum of D_q in the generalized fractal spectrum, $\Delta D_q = D_{qmax} - D_{qmin}$ is the main index to reflect the heterogeneity of pore distribution in the whole aperture range, and $H = (1 + D_2)/2$. This is the Hurst index [37–39], which can characterize the pore connectivity [43]. All of the above-mentioned parameters can be directly extracted from the generalized fractal spectra, and their specific values for organic and inorganic shale pores are listed in Tables 2 and 3, respectively. The results show that for both the organic pores and the inorganic pores of the six shale samples, the following relation is available: $D_0 > D_1 > D_2$, which means that the structures of the organic and inorganic pores are in accordance with the multifractal characteristics.

Table 2. Characteristic parameters from generalized fractal spectra of organic shale pores.

Shale No.	D_0	D_1	D_2	D_{qmax}	D_{qmin}	ΔD_q	$D_0 - D_1$	H
SC-1	1.000	0.986	0.975	1.071	0.868	0.204	0.014	0.988
SC-2	1.000	0.978	0.960	1.122	0.850	0.272	0.022	0.890
CQ-1	1.000	0.989	0.982	1.202	0.962	0.240	0.011	0.991
CQ-2	1.000	0.986	0.977	1.251	0.954	0.297	0.014	0.989
JX-1	1.000	0.995	0.991	1.029	0.959	0.070	0.005	0.996
JX-2	1.000	0.994	0.989	1.025	0.944	0.081	0.006	0.995

Table 3. Characteristic parameters from generalized fractal spectra of inorganic shale pores.

Shale No.	D_0	D_1	D_2	D_{qmax}	D_{qmin}	ΔD_q	$D_0 - D_1$	H
SC-1	1.000	0.880	0.726	1.071	0.475	0.697	0.120	0.863
SC-2	1.000	0.777	0.555	1.122	0.335	1.169	0.223	0.778
CQ-1	1.000	0.827	0.639	1.202	0.407	0.821	0.173	0.820
CQ-2	1.000	0.701	0.485	1.251	0.297	1.060	0.299	0.743
JX-1	1.000	0.775	0.555	1.029	0.334	0.932	0.225	0.777
JX-2	1.000	0.917	0.821	1.025	0.572	0.572	0.083	0.911

Figure 5 illustrates the multifractal spectra (the relationship between $f(\alpha)$ and α of organic and inorganic shale pores, which provide bases for evaluating the heterogeneity of

the PSD in terms of trend and symmetry. Unlike the generalized fractal spectra, in the multifractal spectra, smaller α mainly reflects the heterogeneity of adsorption pores, while greater α mainly reflects the heterogeneity of seepage pores. It can be seen from Figure 5 that the multifractal spectra of both the organic and the inorganic pores show obvious asymmetry. For the inorganic pores of all the samples and the organic pores of the samples from the Jiurui Basin, the positive-slope part of the multifractal spectra is wider and longer than the negative-slope part, while for the organic pores of the samples from the Longmaxi and Niutitang shales the opposite is true. This phenomenon also indicates that the structures of the organic and inorganic pores are in accordance with the multifractal characteristics. To comprehensively analyze the multifractal spectra, several characteristic parameters denoted as α_0, α_{max}, α_{min}, $\alpha_0 - \alpha_{min}$, $\alpha_{max} - \alpha_0$, $\Delta\alpha$ and R were also introduced in this study, where α_0 is the value of α corresponding to the maximum $f(\alpha)$, α_{max} and $\alpha_{\min}$ are the maximum and minimum of α in the multifractal spectra, $\Delta\alpha = \alpha_{max} - \alpha_{min}$, which represents the degree of variation in the distribution of pores with different sizes, and $R = (\alpha_0 - \alpha_{min}) - (\alpha_{max} - \alpha_0)$, which is the deviation of the multifractal spectra. All of the above-mentioned parameters can be directly extracted from the multifractal spectra, and their specific values for organic and inorganic shale pores are listed in Tables 4 and 5, respectively.

Table 4. Characteristic parameters from generalized fractal spectra of inorganic shale pores.

Shale No.	α_0	α_{max}	α_{min}	$\alpha_0 - \alpha_{min}$	$\alpha_{max} - \alpha_0$	$\Delta\alpha$	R
SC-1	1.014	0.371	0.946	0.068	0.357	0.425	−0.289
SC-2	1.008	1.220	0.946	0.062	0.212	0.274	−0.150
CQ-1	1.013	1.667	0.880	0.133	0.654	0.787	−0.521
CQ-2	1.026	2.291	0.844	0.182	1.265	1.447	−1.083
JX-1	1.006	1.055	0.906	0.100	0.049	0.149	0.051
JX-2	1.003	1.060	0.935	0.068	0.057	0.125	0.011

Table 5. Characteristic parameters from multifractal spectra of inorganic shale pores.

Shale No.	α_0	α_{max}	α_{min}	$\alpha_0 - \alpha_{min}$	$\alpha_{max} - \alpha_0$	$\Delta\alpha$	R
SC-1	1.127	1.273	0.371	0.756	0.146	0.902	0.610
SC-2	1.224	1.420	0.268	0.956	0.196	1.152	0.760
CQ-1	1.243	1.498	0.211	1.032	0.255	1.287	0.777
CQ-2	1.095	1.462	0.234	0.861	0.367	1.228	0.494
JX-1	1.149	1.320	0.308	0.841	0.171	1.012	0.670
JX-2	1.062	1.179	0.518	0.544	0.117	0.661	0.427

4. Discussion

4.1. Comparison of Multifractal Parameters between Organic and Inorganic Shale Pores

Figure 6 compares the values of D_0–D_1, ΔD_q and H between the organic and inorganic shale pores. Based on Liu et al. [15] and Song et al. [44], the value of D_0–D_1 can describe the uniformity of the PSD, and higher values for D_0–D_1 correspond to less uniformity. Therefore, the results of Figure 6a prove that the size distribution of the organic shale pores has much greater uniformity than that of the inorganic pores. From Figure 6b, it can be seen that the inorganic pores of our samples have higher ΔD_q values, with an average of 0.875, compared to the organic pores, which have an average value of 0.194. This demonstrates that the heterogeneity of the inorganic pore distribution in the whole aperture range is much stronger than for the organic pores. Additionally, Figure 6c shows that the H values of the organic pores, which approach 1.0, are higher than those of the inorganic pores. This signifies that the organic pores have better connectivity compared with the inorganic pores, according to the physical meaning of H.

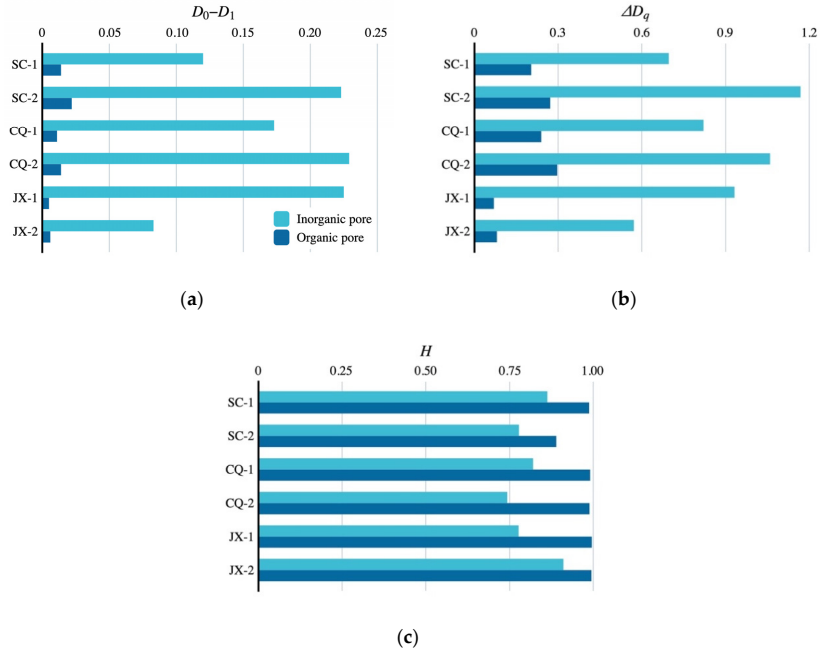

Figure 6. Comparison of the characteristic parameters from generalized fractal spectra between organic and inorganic pores: (**a**) $D_0 - D_1$, (**b**) ΔD_q, (**c**) H.

Figure 7 compares the values of $\Delta\alpha$ and R between the organic and inorganic shale pores. Similar to ΔD_q, $\Delta\alpha$ is another main parameter to evaluate the heterogeneity of the PSD in multifractal theory. As shown in Figure 7a, for the CQ-2 sample, the $\Delta\alpha$ value of the organic pores is higher than that of the inorganic pores, while for other samples used in the study the opposite is true. These data signify the fact that the organic pores of the CQ-2 sample are more heterogeneous than the inorganic pores, while, for all the other samples, the inorganic pores are more heterogeneous than the organic pores. On average, it is apparent that the size distribution of the inorganic pores in our samples has a higher $\Delta\alpha$ value compared with that of the organic pores, indicating that the inorganic shale pores possess more obvious multifractal characteristics than the organic pores. Additionally, Song et al. [44] pointed out that the positive-slope part of the multifractal spectra represents the concentrated areas of the pore volume distribution, while the negative-slope part represents the sparse areas of the pore volume distribution. In this case, it can be inferred from Figure 7b that the size distributions of the organic pores of the samples from the Longmaxi and Niutitang shales are dominated by concentrated areas because of the negative R values, while the size distribution of the inorganic pores of all samples and the organic pores of samples from the Jiurui Basin are dominated by sparse areas because of the positive R values.

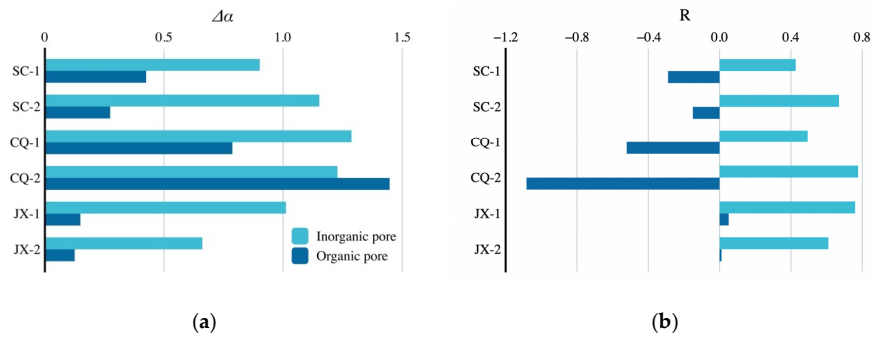

Figure 7. Comparison of characteristic parameters from multifractal spectrums between organic and inorganic pores: (**a**) $\Delta\alpha$, (**b**) R.

4.2. Method Comparison

In this section, we compare the multifractal characteristics of shale pores obtained using NMR with those obtained using scanning electron microscopy (SEM). Table 6 lists the average values and variances of $\Delta\alpha$ for both organic and inorganic shale pores obtained using NMR and SEM in this study [17]. The results show that, compared to SEM, the $\Delta\alpha$ values obtained by NMR are lower for both organic and inorganic pores. This difference may be due to the fact that the research scale of SEM is very small, which could lead to the investigated pores exhibiting more obvious multifractal characteristics. Furthermore, we conducted a variance analysis between the $\Delta\alpha$ values of the organic and inorganic pores. The results indicate that the F value of the variance analysis is 4.746, which is higher than the threshold (4.28), indicating that the separate studies on the multifractal characteristics of the organic and inorganic shale pores have statistical significance. In other words, the variation in $\Delta\alpha$ values between the two types of pores is not due to chance but rather reflects a real difference in the multifractal characteristics of the two types of pores.

Table 6. The average values and variances of $\Delta\alpha$ for organic and inorganic shale pores obtained using NMR and SEM.

Value	NMR		SEM	
	Organic Pores	Inorganic Pores	Organic Pores	Inorganic Pores
Average value	0.535	1.040	1.475	1.519
Variance	0.045	0.215	0.100	0.130
F value (ANOVA)	4.746		1.160	

4.3. Geological Significance of Multifractal Characteristics of Organic and Inorganic Shale Pores

To evaluate the geological significance of the multifractal characteristics of organic and inorganic shale pores, we analyzed the impacts of multifractal characteristic parameters (H and $\Delta\alpha$) on permeability, Langmuir parameters and irreducible water saturation by conducting the experiments reported in this section.

4.3.1. Impacts on Permeability

Shale permeability is one of the most critical parameters for studying fluid migration in shale reservoirs. This paper investigated the impacts of the multifractal characteristics of organic and inorganic shale pores on shale permeability through experiments, and the results are depicted in Figure 8. It can be seen from Figure 8 that, compared to organic pores, shale permeability has a closer relationship with the multifractal characteristics of inorganic pores. Additionally, shale permeability increases with the value of H for inorganic pores but decreases with the value of $\Delta\alpha$ for inorganic pores. This signifies that stronger inhomogeneity and worse connectivity of inorganic pores correspond to lower shale permeability.

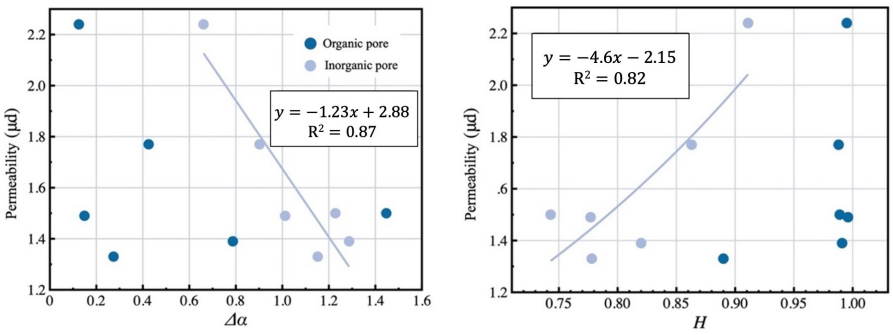

Figure 8. The relationships between multifractal characteristic parameters of organic and inorganic pores and permeability.

4.3.2. Impacts on Langmuir Parameters

The Langmuir parameters of shale (Langmuir pressure constant and Langmuir volume constant) are critical for evaluating and calculating shale gas content in reservoirs. This paper investigates the impacts of the multifractal characteristics of organic and inorganic shale pores on Langmuir parameters through gas adsorption experiments. The experimental equipment and the test system are shown in Figure 9. To ensure safety, CO_2 was used in this experiment. The results of the gas adsorption experiment are listed in Table 7, and the relationships between the Langmuir parameters and the multifractal characteristics of organic and inorganic shale pores are depicted in Figures 10 and 11. It can be found in Figure 10 that the value of $\Delta\alpha$ for organic pores has an obvious impact on the Langmuir pressure constant and the Langmuir volume constant. As $\Delta\alpha$ increases, the Langmuir pressure constant tends to decrease, and the Langmuir volume constant tends to increase. This signifies that the stronger inhomogeneity of organic pores corresponds to better adsorption properties of shale. The principal reason for this conclusion is that the more inhomogeneous the organic pore structure, the more irregular the pore surface, which increases the contact area between the adsorbed gas and the organic pore surface and further increases the adsorption capacity of shale. Therefore, the $\Delta\alpha$ of organic pores can be an indicator for evaluating shale reservoir quality. Additionally, the results reported in Figure 11 indicate that there are no obvious relationships between the Langmuir parameters of shale and the multifractal characteristics of inorganic pores.

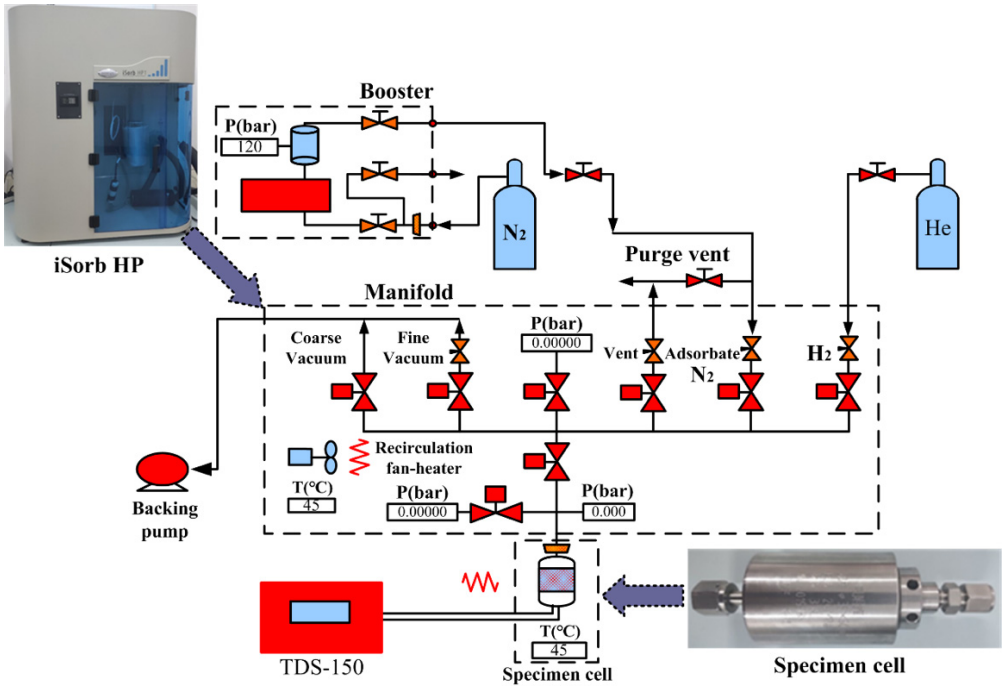

Figure 9. Schematic of the gas adsorption test system (the figure has been adapted from a Shandong University of Science and Technology introduction to test systems in gas diffusion dynamics).

Table 7. Langmuir parameters of shale samples.

Shale No.	SC-1	SC-2	CQ-1	CQ-2	JX-1	JX-2
Langmuir pressure constant (MPa)	11.41	11.54	8.02	3.77	12.59	10.81
Langmuir volume constant (m^3/kg)	2.42	1.06	2.03	3.63	1.35	1.01

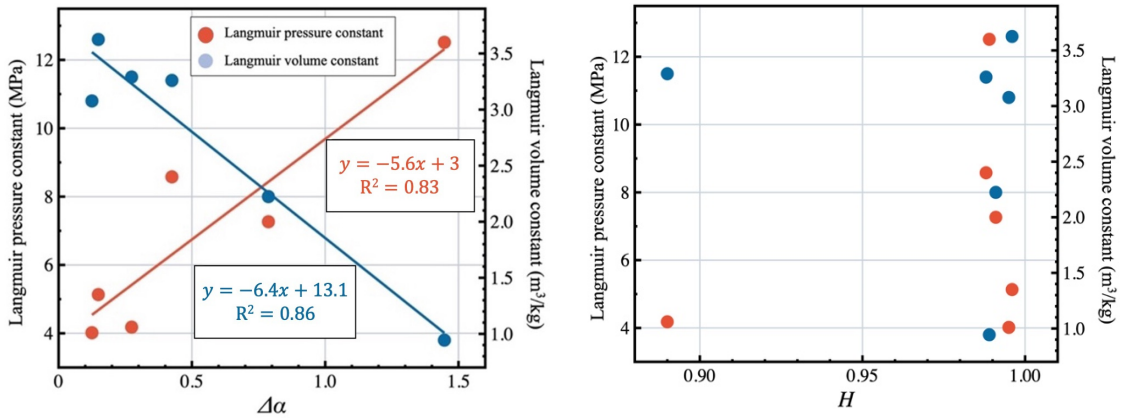

Figure 10. The relationships between multifractal characteristic parameters of organic pores and Langmuir parameters.

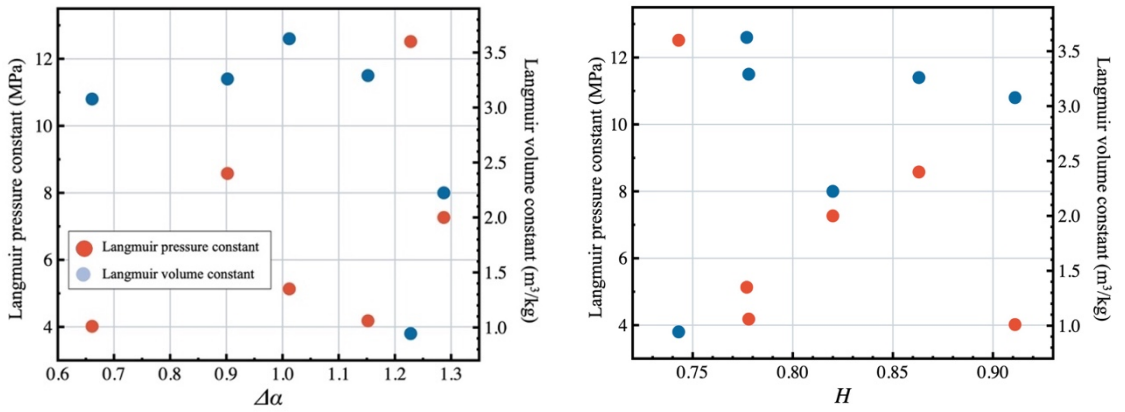

Figure 11. The relationships between multifractal characteristic parameters of inorganic pores and Langmuir parameters.

4.3.3. Impacts on Irreducible Water Saturation

The irreducible water saturation of shale is a critical factor in revealing the spontaneous imbibition mechanism of fracturing fluid and the backflow mechanism of gas–water two-phase flow in shale reservoirs. In this study, the value of the irreducible water saturation of shale was determined by nuclear magnetic resonance test, and the impacts of multifractal characteristics of organic and inorganic shale pores on irreducible water saturation were investigated. The results, shown in Figure 12, indicate that the multifractal characteristics of both organic and inorganic pores have a clear impact on irreducible water saturation, with the impact of multifractal characteristics of inorganic pores being particularly evident. This is because water adsorption mainly occurs in inorganic shale matter. Additionally, the irreducible water saturation of shale increases with the value of $\Delta\alpha$ for both organic and inorganic pores but decreases with the value of H for inorganic pores. This signifies that stronger inhomogeneity of both organic and inorganic pores and worse connectivity of inorganic pores correspond to higher irreducible water saturation in shale. The principal reason for this conclusion is that stronger inhomogeneity and worse connectivity of shale pores mean that the fluid seepage channel is more tortuous, making it more difficult for water to outflow from the shale reservoir, which increases the irreducible water saturation of the shale. Therefore, $\Delta\alpha$ of both organic and inorganic pores and H of inorganic pores can be used as indicators for estimating the irreducible water saturation of shale. Additionally, considering the close relationship between the flowback rate of fracturing fluid and irreducible water saturation in shale gas production, the above parameters can also be used as indicators for estimating the flowback rate of fracturing fluid.

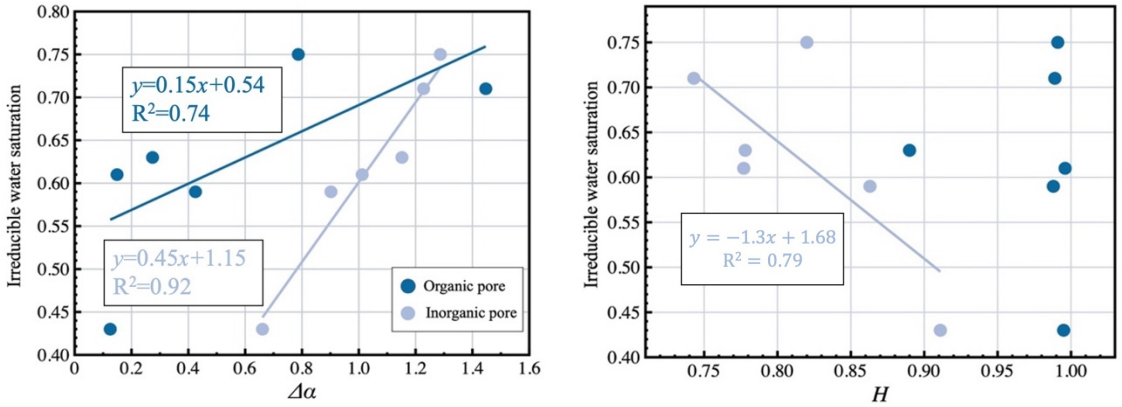

Figure 12. The relationships between multifractal characteristic parameters of organic and inorganic pores and irreducible water saturation.

5. Conclusions

In this study, the multifractal characteristics of organic and inorganic shale pores were separately analyzed and evaluated using a new NMR-based method. This method acquires the PSD of organic and inorganic shale pores separately on a laboratory scale, rather than a microscale. Thus, the test results can better represent the pore structure of underground shale. On the basis of the results from this study, the following four major conclusions are drawn:

(1) Through NMR experiments on shale samples under water- and kerosene-saturated conditions, respectively, the size distributions of organic and inorganic shale pores were obtained. On balance, the size of organic pores is smaller than inorganic pores.

(2) The structures of both organic and inorganic shale pores possess multifractal characteristics. Compared with organic pores, inorganic shale pores generally have greater values for D_0–D_1, ΔDq and $\Delta\alpha$, but a smaller value for H. These data indicate that inorganic shale pores possess stronger heterogeneity and poorer connectivity than organic pores.

(3) The geological significance of the multifractal characteristics of inorganic shale pores was investigated by multifractal characteristic parameters ($\Delta\alpha$ and H). The results showed that the multifractal characteristics of inorganic pores have a significant impact on shale permeability and irreducible water saturation. The stronger inhomogeneity of inorganic pores corresponds to lower shale permeability and higher irreducible water saturation. The better connectivity of inorganic pores corresponds to higher shale permeability and lower irreducible water saturation. The principal reason for this phenomenon is that the multifractal characteristics of inorganic pores control the tortuosity of shale seepage channels to a certain extent. Additionally, the $\Delta\alpha$ of inorganic pores can be an indicator for estimating the irreducible water saturation of shale and the flowback rate of fracturing fluid.

(4) The geological significance of the multifractal characteristics of organic shale pores was also investigated using multifractal characteristic parameters ($\Delta\alpha$ and H). The results showed that the multifractal characteristics of organic pores have a significant impact on the adsorption capacity of shale, and have a weak impact on irreducible water saturation. The stronger inhomogeneity of organic pores corresponds to the stronger adsorption capacity of shale (lower Langmuir pressure constant and higher Langmuir volume constant) and higher irreducible water saturation. The principal reason for this phenomenon is that the multifractal characteristics of organic pores control the contact area between the fluid and the surface of organic pores to a certain extent. Additionally, the $\Delta\alpha$ of organic pores can be an indicator for evaluating shale reservoir quality.

It should be noted that the conclusions mentioned above were reached under laboratory conditions, which may not accurately reflect in situ reservoir conditions due to depressurization. This depressurization reduces the effective stress on the shale, leading to changes in porosity and permeability. To accurately acquire the PSD of shale under in situ reservoir conditions, further investigation is necessary. Additionally, the presence of clay and magnetic minerals in shale may affect the PSD, porosity and permeability measured by NMR due to signal distortion. These experimental biases need to be further clarified in future studies.

Author Contributions: Conceptualization, methodology, writing—review and editing, R.Y.; funding acquisition, W.L.; writing—original draft preparation, L.M. All authors have read and agreed to the published version of the manuscript.

Funding: This research was funded by the National Natural Science Foundation of China (No. 42177124), the Natural Science Foundation of Jiangsu Province (No. BK20180636), the Natural Science Foundation of Liaoning Province (No. 2020KF2303), the Natural Science Foundation of Shandong Province (No. ZR2022ME195) and the National Natural Science Foundation of China (grant no. 51574156).

Institutional Review Board Statement: Not applicable.

Informed Consent Statement: Not applicable.

Data Availability Statement: Data associated with this research are available and can be obtained upon reasonable request to the corresponding author.

Acknowledgments: The authors would like to thank the anonymous reviewers for their valuable comments and suggestions, which helped improve the quality of the paper.

Conflicts of Interest: The authors declare no conflict of interest.

Appendix A

Table A1. Mineral composition of the shale samples from XRD analysis.

Shale No.	Quartz (%)	Feldspar (%)	Calcite (%)	Dolomite (%)	Clays (%)	Pyrite (%)
SC-1	32.8	11.1	5.2	6.4	40.7	3.6
SC-2	41.9	8.2	4.0	2.1	38.6	2.7
CQ-1	30.4	5.2	12.9	2.1	47.9	0
CQ-2	26.3	12.1	2.4	9.0	46.2	2.0
JX-1	22.2	5.5	8.1	1.9	56.9	3.4
JX-2	19.1	0	13.0	1.3	61.4	2.2

Table A2. TOC content and Ro of the shale samples.

Shale No.	SC-1	SC-2	CQ-1	CQ-2	JX-1	JX-2
TOC (%)	2.38	2.51	1.21	1.35	0.62	0.58
Ro (%)	0.51	0.72	2.12	1.98	3.15	3.21

References

1. Guo, M.; Lu, X.; Nielsen, C.P.; McElroy, M.B.; Shi, W.; Chen, Y.; Xu, Y. Prospects for shale gas production in China: Implications for water demand. *Renew. Sustain. Energy Rev.* **2016**, *66*, 742–750. [CrossRef]
2. Hu, Q.; Zhang, Y.; Meng, X.; Li, Z.; Xie, Z.; Li, M. Characterization of micro-nano pore networks in shale oil reservoirs of Paleogene Shahejie Formation in Dongying Sag of Bohai Bay Basin, East China. *Pet. Explor. Dev.* **2017**, *44*, 720–730. [CrossRef]
3. Liu, K.; Ostadhassan, M.; Kong, L. Fractal and Multifractal Characteristics of Pore Throats in the Bakken Shale. *Transp. Porous Media* **2019**, *126*, 579–598. [CrossRef]
4. Javadpour, F.; Fisher, D.; Unsworth, M. Nanoscale Gas Flow in Shale Gas Sediments. *J. Can. Pet. Technol.* **2007**, *46*, 55–61. [CrossRef]
5. Xi, Z.; Tang, S.; Wang, J.; Yi, J.; Guo, Y.; Wang, K. Pore Structure and Fractal Characteristics of Niutitang Shale from China. *Minerals* **2018**, *8*, 163. [CrossRef]
6. Zhang, T.; Li, X.; Li, J.; Feng, D.; Wu, K.; Shi, J.; Sun, Z.; Han, S. A Fractal Model for Gas–Water Relative Permeability in Inorganic Shale with Nanoscale Pores. *Transp. Porous Media* **2018**, *122*, 305–331. [CrossRef]

7. Schmitt Rahner, M.; Halisch, M.; Peres Fernandes, C.; Weller, A.; Sampaio Santiago dos Santos, V. Fractal dimensions of pore spaces in unconventional reservoir rocks using X-ray nano- and micro-computed tomography. *J. Nat. Gas Sci. Eng.* **2018**, *55*, 298–311. [CrossRef]
8. Peng, N.; He, S.; Hu, Q.; Zhang, B.; He, X.; Zhai, G.; He, C.; Yang, R. Organic nanopore structure and fractal characteristics of Wufeng and lower member of Longmaxi shales in southeastern Sichuan, China. *Mar. Pet. Geol.* **2019**, *103*, 456–472. [CrossRef]
9. Ji, W.; Song, Y.; Jiang, Z.; Meng, M.; Liu, Q.; Chen, L.; Wang, P.; Gao, F.; Huang, H. Fractal characteristics of nano-pores in the Lower Silurian Longmaxi shales from the Upper Yangtze Platform, south China. *Mar. Pet. Geol.* **2016**, *78*, 88–98. [CrossRef]
10. Jiang, F.; Chen, D.; Chen, J.; Li, Q.; Liu, Y.; Shao, X.; Hu, T.; Dai, J. Fractal Analysis of Shale Pore Structure of Continental Gas Shale Reservoir in the Ordos Basin, NW China. *Energy Fuels* **2016**, *30*, 4676–4689. [CrossRef]
11. Yang, F.; Ning, Z.; Liu, H. Fractal characteristics of shales from a shale gas reservoir in the Sichuan Basin, China. *Fuel* **2014**, *115*, 378–384. [CrossRef]
12. Zhang, L.; Li, J.; Tang, H.; Guo, J. Fractal Pore Structure Model and Multilayer Fractal Adsorption in Shale. *Fractals* **2014**, *22*, 1440010. [CrossRef]
13. Li, A.; Ding, W.; He, J.; Dai, P.; Yin, S.; Xie, F. Investigation of pore structure and fractal characteristics of organic-rich shale reservoirs: A case study of Lower Cambrian Qiongzhusi formation in Malong block of eastern Yunnan Province, South China. *Mar. Pet. Geol.* **2016**, *70*, 46–57. [CrossRef]
14. Starzewski, M. Continuum mechanics models of fractal porous media: Integral relations and extremum principles. *J. Mech. Mater. Struct.* **2009**, *4*, 901–912. [CrossRef]
15. Liu, K.; Ostadhassan, M.; Zou, J.; Gentzis, T.; Rezaee, R.; Bubach, B.; Carvajal-Ortiz, H. Multifractal analysis of gas adsorption isotherms for pore structure characterization of the Bakken Shale. *Fuel* **2018**, *219*, 296–311. [CrossRef]
16. Liu, K.; Ostadhassan, M.; Sun, L.; Zou, J.; Yuan, Y.; Gentzis, T.; Zhang, Y.; Carvajal-Ortiz, H.; Rezaee, R. A comprehensive pore structure study of the Bakken Shale with SANS, N2 adsorption and mercury intrusion. *Fuel* **2019**, *245*, 274–285. [CrossRef]
17. Wang, P.; Jiang, Z.; Ji, W.; Zhang, C.; Yuan, Y.; Chen, L.; Yin, L. Heterogeneity of intergranular, intraparticle and organic pores in Longmaxi shale in Sichuan Basin, South China: Evidence from SEM digital images and fractal and multifractal geometries. *Mar. Pet. Geol.* **2016**, *72*, 122–138. [CrossRef]
18. Sun, W.; Zuo, Y.; Wu, Z.; Liu, H.; Xi, S.; Shui, Y.; Wang, J.; Liu, R.; Lin, J. Fractal analysis of pores and the pore structure of the Lower Cambrian Niutitang shale in northern Guizhou province: Investigations using NMR, SEM and image analyses. *Mar. Pet. Geol.* **2019**, *99*, 416–428. [CrossRef]
19. Guan, M.; Liu, X.; Jin, Z.; Lai, J. The heterogeneity of pore structure in lacustrine shales: Insights from multifractal analysis using N2 adsorption and mercury intrusion. *Mar. Pet. Geol.* **2020**, *114*, 104150. [CrossRef]
20. Chen, F.; Lu, S.; Ding, X. Pore Types and Quantitative Evaluation of Pore Volumes in the Longmaxi Formation Shale of Southeast Chongqing, China. *Acta Geol. Sin. Engl. Ed.* **2018**, *92*, 342–353. [CrossRef]
21. Wu, J.; Yuan, Y.; Niu, S.; Wei, X.; Yang, J. Multiscale characterization of pore structure and connectivity of Wufeng-Longmaxi shale in Sichuan Basin, China. *Mar. Pet. Geol.* **2020**, *120*, 104514. [CrossRef]
22. Zhang, W.; Huang, Z.; Li, X.; Chen, J.; Guo, X.; Pan, Y.; Liu, B. Estimation of organic and inorganic porosity in shale by NMR method, insights from marine shales with different maturities. *J. Nat. Gas Sci. Eng.* **2020**, *78*, 103290. [CrossRef]
23. Zhou, S.; Yan, G.; Xue, H.; Guo, W.; Li, X. 2D and 3D nanopore characterization of gas shale in Longmaxi formation based on FIB-SEM. *Mar. Pet. Geol.* **2016**, *73*, 174–180. [CrossRef]
24. Miao, Y.; Li, X.; Lee, J.; Zhou, Y.; Liu, S.; Chang, Y.; Wang, S. Characterization of hydrocarbon/pores generation and methane adsorption in shale organic matter. *Pet. Sci. Technol.* **2018**, *36*, 1187–1193. [CrossRef]
25. Sun, Z.; Li, X.; Shi, J.; Zhang, T.; Sun, F. Apparent permeability model for real gas transport through shale gas reservoirs considering water distribution characteristic. *Int. J. Heat Mass Transf.* **2017**, *115*, 1008–1019. [CrossRef]
26. Li, J.; Li, X.; Wang, X.; Li, Y.; Wu, K.; Shi, J.; Yang, L.; Feng, D.; Zhang, T.; Yu, P. Water distribution characteristic and effect on methane adsorption capacity in shale clay. *Int. J. Coal Geol.* **2016**, *159*, 135–154. [CrossRef]
27. Li, A.; Ding, W.; Jiu, K.; Wang, Z.; Wang, R.; He, J. Investigation of the pore structures and fractal characteristics of marine shale reservoirs using NMR experiments and image analyses: A case study of the Lower Cambrian Niutitang Formation in northern Guizhou Province, South China. *Mar. Pet. Geol.* **2018**, *89*, 530–540. [CrossRef]
28. Zhang, J.; Li, X.; Zou, X.; Li, J.; Xie, Z.; Wang, F. Characterization of multi-type pore structure and fractal characteristics of the Dalong Formation marine shale in northern Sichuan Basin. *Energy Sources Part A Recovery Util. Environ. Eff.* **2020**, *42*, 2764–2777. [CrossRef]
29. Liu, Z.; Liu, D.; Cai, Y.; Yao, Y.; Pan, Z.; Zhou, Y. Application of nuclear magnetic resonance (NMR) in coalbed methane and shale reservoirs: A review. *Int. J. Coal Geol.* **2020**, *218*, 103261. [CrossRef]
30. Liu, D.; Ge, H.; Liu, J.; Shen, Y.; Wang, Y.; Liu, Q.; Jin, C.; Zhang, Y. Experimental investigation on aqueous phase migration in unconventional gas reservoir rock samples by nuclear magnetic resonance. *J. Nat. Gas Sci. Eng.* **2016**, *36*, 837–851. [CrossRef]
31. Yao, Y.; Liu, D. Comparison of low-field NMR and mercury intrusion porosimetry in characterizing pore size distributions of coals. *Fuel* **2012**, *95*, 152–158. [CrossRef]
32. Wang, L.; Fu, Y.; Li, J.; Sima, L.; Wu, Q.; Jin, W.; Wang, T. Mineral and pore structure characteristics of gas shale in Longmaxi formation: A case study of Jiaoshiba gas field in the southern Sichuan Basin, China. *Arab. J. Geosci.* **2016**, *9*, 733. [CrossRef]

33. Liu, K.; Ostadhassan, M.; Kong, L. Multifractal characteristics of Longmaxi Shale pore structures by N2 adsorption: A model comparison. *J. Pet. Sci. Eng.* **2018**, *168*, 330–341. [CrossRef]
34. Luo, Q.; Hao, J.; Skovsted, C.B.; Xu, Y.; Liu, Y.; Wu, J.; Zhang, S.; Wang, W. Optical characteristics of graptolite-bearing sediments and its implication for thermal maturity assessment. *Int. J. Coal Geol.* **2018**, *195*, 386–401. [CrossRef]
35. Luo, Q.; Fariborz, G.; Zhong, N.; Wang, Y.; Qiu, N.; Skovsted, C.B.; Suchý, V.; Hemmingsen Schovsbo, N.; Morga, R.; Xu, Y.; et al. Graptolites as fossil geo-thermometers and source material of hydrocarbons: An overview of four decades of progress. *Earth-Sci. Rev.* **2020**, *200*, 103000. [CrossRef]
36. Li, J.; Jin, J.; Wang, L.; Wu, Q.; Lu, J.; Hao, S. Quantitative evaluation of organic and inorganic pore size distribution by NMR:A case from the Silurian Longmaxi Formation gas shale in Fuling area, Sichuan Basin. *Oil Gas Geol.* **2016**, *37*, 129–134.
37. Agboola, O.; Onyango, M.S.; Popoola, P.; Oyewo, O.A. Fractal Geometry and Porosity. In *Fractal Analysis: Applications in Physics, Engineering and Technology*; Brambila, F., Ed.; IntechOpen: London, UK, 2017. [CrossRef]
38. Mandelbrot, B.B. *The Fractal Geometry of Nature*, 1st ed.; W.H. Freeman and Company: San Francisco, CA, USA, 1982; 34p, ISBN 978-0716711865.
39. Mandelbrot, B.B.; Passoja, D.E.; Paulay, A.J. Fractal character of fracture surfaces of metals. *Nature* **1984**, *308*, 721–722. [CrossRef]
40. De Gennes, P.G. Partial filling of a fractal structure, by a wetting fluid. In *Physics of Disordered Materials*; Adler, D., Frizsche, H., Ovshinsky, S.R., Eds.; Plenum Press: New York, NY, USA, 1985; pp. 227–241.
41. Turcotte, D.L. Fractals and fragmentation. *J. Geophys. Res.* **1986**, *91*, 1921–1926. [CrossRef]
42. Sumantri, Y.; Permadi, P. A Study of Sandstone Permeability Anisotropy Through Fractal Concept. *Am. J. Sci. Eng. Technol.* **2018**, *3*, 34–45. [CrossRef]
43. San José Martínez, F.; Martín, M.A.; Caniego, F.J.; Tuller, M.; Guber, A.; Pachepsky, Y.; García-Gutiérrez, C. Multifractal analysis of discretized X-ray CT images for the characterization of soil macropore structures. *Geoderma* **2010**, *156*, 32–42. [CrossRef]
44. Yu, S.; Jiang, B.; Shao, P.; Wu, J. Matrix compression and multifractal characterization for tectonically deformed coals by Hg porosimetry. *Fuel* **2018**, *211*, 661–675. [CrossRef]

Disclaimer/Publisher's Note: The statements, opinions and data contained in all publications are solely those of the individual author(s) and contributor(s) and not of MDPI and/or the editor(s). MDPI and/or the editor(s) disclaim responsibility for any injury to people or property resulting from any ideas, methods, instructions or products referred to in the content.